

## Chapter 2

# Low Correlated Systems: Gases and Dilute Solutions

The Kinematic Theory covers any description of the X-ray scattering process by a distribution of electrons where rescattering (with phase coherence) of the already scattered waves by the distribution has negligible effects. In other words, the scattered radiation is composed by photons that interacted once with the sample. Under these conditions, the scattered intensity, often called the kinematic intensity, is proportional to the form factor square module, (1.25). Material samples in a gaseous, liquid, or solid state are nothing more than atom systems with different degrees of correlation between the atomic positions, ranging from disperse systems, such as a gas, until strongly correlated systems as in a crystals. The Kinematic Theory describes very accurately the X-ray scattering by any of these systems, except only by highly perfect crystals with dimensions larger than a few microns. In this chapter we will begin in fact to discuss analysis methods of atomic systems by kinematic scattering of X-rays starting with the disperse system of lowest possible degree of correlation.

### 2.1 Monatomic Gas

By considering a discrete distribution of  $N$  atoms, as in (1.51), we come to the general expression of kinematic intensity

$$\begin{aligned}
 I(\mathbf{Q}) &= I_{Th} \left| \sum_{a=1}^N f_a(\mathbf{Q}) e^{i\mathbf{Q} \cdot \mathbf{r}_a} \right|^2 = I_{Th} \sum_{a=1}^N \sum_{b=1}^N f_a(\mathbf{Q}) f_b^*(\mathbf{Q}) e^{i\mathbf{Q} \cdot (\mathbf{r}_a - \mathbf{r}_b)} = \\
 &= I_{Th} \sum_{a=1}^N |f_a(\mathbf{Q})|^2 + I_{Th} \sum_{a=1}^N \sum_{b \neq a}^N f_a(\mathbf{Q}) f_b^*(\mathbf{Q}) e^{i\mathbf{Q} \cdot \mathbf{r}_{ab}} \quad (2.1)
 \end{aligned}$$

where  $\mathbf{r}_{ab} = \mathbf{r}_a - \mathbf{r}_b$  and  $f_b^*(Q) \neq f_b(Q)$  when the resonance amplitudes are taken into account, (1.60). At first this expression of intensity is valid for any type of sample scattering within the kinematic regime being especially useful in cases where it is feasible to discretize the electronic density atom-by-atom.

In the case of monatomic gas,  $f_a(Q) = f_b(Q) = f(Q)$  and the  $\mathbf{r}_{ab}$  separations between pairs of atoms vary continuously over time so that

$$I(Q) = \left[ N + \sum_{a=1}^N \sum_{b \neq a}^N \cos(\mathbf{Q} \cdot \mathbf{r}_{ab}) \right] I_{Th} |f(Q)|^2 \quad (2.2)$$

corresponds to the instantaneous intensity scattered by the system. The coherent scattering cross-section of an atom, e.g. Fig. 1.11, has very small values, reaching at most a few thousand barns,  $\sim 10^{-25} \text{ m}^2$ . The scattered intensities are so weak that the intensity measures are in most cases done in relatively long times compared to the average time that the atoms in the gas take to move through the dimensions of the illuminated volume by the X-ray beam. A measure of  $I(Q)$  therefore contains the temporal average value  $\langle \dots \rangle_t$  of the double summation in (2.2). Since each atom has independent movements—a characteristic of disperse systems<sup>1</sup>—the cosine temporal average is zero, i.e.  $\langle \cos(\mathbf{Q} \cdot \mathbf{r}_{ab}) \rangle_t = 0$  for any pair of atoms, as long as  $Q \neq 0$ , making the term in brackets,  $[\dots]$ , contribute only with one factor of  $N$ . However, when  $Q = 0$ , the double summation is equal to  $N(N - 1)$  and the term in brackets contributes with a factor  $N^2$ . Note that in a random distribution of many atoms, the instantaneous intensity also obeys the relations  $I(Q \neq 0) \propto N$  and  $I(Q = 0) \propto N^2$ , but in this case it is because of the statistical average null value of the cosine in the distribution. How different from zero should the  $\mathbf{Q}$  vector be for the average (temporal or statistical) of the cosine be null? Or, in other words, what is the function  $I(Q)$  in the region where the multiplicative factor (term in brackets) changes from  $N$  to  $N^2$ ? This function depends on shape and size of the gas volume illuminated by radiation or, more specifically, on the volume dimension perpendicular to the beam on the incidence plane. Quantitatively, the volume Fourier transform determines how far from  $Q = 0$  we must look at the scattered radiation for the average of the cosines to be null. For a qualitative description, we can make a simple estimation of the scattering angle  $2\theta$  where the average is no longer null. From the definitions of versor  $\hat{\pi}$  and reciprocal vector  $\mathbf{Q}$ , (1.3) and (1.23), it is easy to verify that

$$\lim_{2\theta \rightarrow 0} \mathbf{Q} = Q\hat{\pi}.$$

If  $D$  is the volume dimension in direction  $\hat{\pi}$ , the vectorial product maximum value will be  $\mathbf{Q} \cdot \mathbf{r}_{ab} = QD$ . For the average cosines to be null we need  $QD \geq 2\pi$ , and thus

---

<sup>1</sup>Ideal gases under normal temperature and pressure conditions stand for ideally disperse systems (Guinier and Fournet 1955).

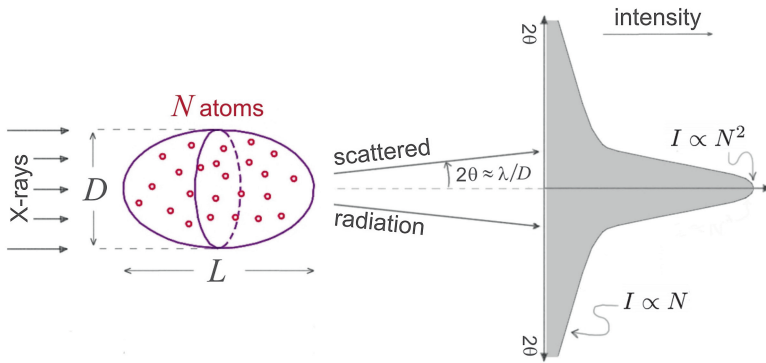


**Fig. 2.1** Ultra-small angle region,  $2\theta < \lambda/D$ , where all the gas atoms scatter in phase,  $I \propto N^2$ . In real situations,  $D$  and  $L$  generally correspond to the transverse and longitudinal coherence lengths of the X-ray beam, as in Fig. 1.4

$$I(Q) = \begin{cases} N I_{Th} |f(Q)|^2 & \text{se } Q \geq 2\pi/D \quad (2\theta \geq \lambda/D) \\ N^2 I_{Th} |f(0)|^2 & \text{se } Q < 2\pi/D \quad (2\theta < \lambda/D) \end{cases} \quad (2.3)$$

as illustrated in Fig. 2.1.

Generally,  $D$  is the smallest value among sample size, beam transverse section, or beam transverse coherence length, (1.16). In practice, the value of  $D$  is large enough for the high intensity region—proportional to  $N^2$ —to be indistinguishable from the direct beam. Away from the direct beam, the intensity is proportional to the number  $N$  of atoms and varies with  $Q$  according to the atomic scattering factor of the element in question, showing that experiments to directly measure  $f(Q)$  are possible, in principle, in monatomic gases.

...

**Exercise 2.1.** Given a pictorial expression of coherent intensity

$$I(Q) = N I_{Th} |f(Q)|^2 [1 + (N - 1) G(Q)]$$

where  $N$  is the number of atoms within the coherence volume  $V \approx D^2 L$ .  $G(Q) = \exp(-Q^2/2\sigma_Q^2)$ , with  $\sigma_Q = \pi/D$ , is an empirical function used here to describe the intensity variation around the direct beam, (2.3). (a) Estimate the relative percentage  $R$  of photons scattered outside the direct beam in relation to the total number of photons scattered by the  $N$  atoms. Note: write the result as a function of volumetric density  $\rho$  of atoms in the sample. (b) Using  $D = 0.04 \mu\text{m}$  and  $L = 0.03 \mu\text{m}$  as the coherence lengths for Cu radiation, Exercise 1.5, what is the value of  $R$  for gas argon (Ar) at standard conditions of temperature and pressure (STP)? (c) If in the

liquefied argon the smaller interatomic distances were in the order of  $3.6 \text{ \AA}$ , what is the value of  $R$ ? (d) Interpret the results.

Answer (a): The scattered intensity outside the direct beam is  $I_1 = N \Phi \sigma_R$ , (1.50). In the ultra-small angle region,<sup>2</sup> the intensity is  $I_2 = 0.5 \pi N(N-1) \Phi r_e^2 |f_{\text{Ar}}(0)|^2 (\lambda/D)^2$ . Since  $N-1 \simeq \varrho V$ ,

$$R = 100 \frac{I_1}{I_1 + I_2} =$$

$$= 100 \frac{\sigma_R}{\sigma_R + 0.5 \pi r_e^2 |f_{\text{Ar}}(0)|^2 (N-1)(\lambda/D)^2} R \simeq 100 \frac{\sigma_R}{\sigma_R + 0.5 \pi r_e^2 |f_{\text{Ar}}(0)|^2 L \lambda^2 \varrho} .$$

Answer (b): For 8 keV photons,  $\sigma_R(\text{Ar}) = 63.9 \text{ barn}$  and  $\lambda = 1.54 \text{ \AA}$ .  $f_{\text{Ar}}(0) = 18$  and  $r_e^2 = 0.0794 \text{ barn}$ . At STP the molar volume of an ideal gas is  $24.467 \text{ L/Mol}$ ,  $\varrho = 2.46 \times 10^7 \text{ atoms}/\mu\text{m}^3$  and  $N = 1.2 \times 10^3$ . Then,

$$R \simeq 100 \frac{63.9}{63.9 + 0.71} = 98.9 \% .$$

Answer (c): In a liquid, assuming that each atom occupies an average free volume of  $46.7 \text{ \AA}^3$ , we have  $\varrho = 2.14 \times 10^{10} \text{ atoms}/\mu\text{m}^3$  and  $N = 1.0 \times 10^6$ , which leads to

$$R \simeq 100 \frac{63.9}{63.9 + 615.7} = 9.4 \% .$$

Answer (d): The results in (b) and (c) show that measurable coherent intensity from disperse systems only occurs because the X-ray beam is not a perfect plane wave (infinity coherence lengths). Otherwise, the coherence volume would be as extensive as the macroscopic dimensions of the total illuminated volume by the X-ray beam, of the order of  $1 \text{ mm}^3$ , containing about  $10^{16}$  atoms (Ar gas) and resulting in  $R = 0$ , which means a completely destructive interference outside the direct beam. On the other hand, even with beams of finite coherence, liquid or solid samples where the atom density varies between  $10^{10}$  and  $10^{11} \text{ atoms}/\mu\text{m}^3$  have values of  $R$  practically null in the absence of constructive interferences (diffraction) produced by correlation of atomic positions in the sample. The use of X-ray equipment with focusing optics, providing high flux and low coherence, is therefore ideal for the study of low correlated systems.

...

---

<sup>2</sup>With  $Q = (4\pi/\lambda) \sin(\gamma/2)$ ,  $\int G(Q) d\Omega = 2\pi \int \exp\{-\alpha \sin^2(\gamma/2)\} \sin \gamma d\gamma \simeq 4\pi/\alpha = 0.5 \pi (\lambda/D)^2$ .

## 2.2 Dispersed Molecules: Random Orientations

Similar to the case of monatomic gas, the scattering by a gas of identical molecules is independent of the mutual interference between molecules,<sup>3</sup> containing only internal structure information of the molecule. Other disperse molecular systems, such as low concentration solutions, may also exhibit scatterings free from mutual interference. Unlike atoms, molecules are 3-D structures that, in general, do not have spherical symmetry. Intensity measurements in such systems thus correspond to the sum of the scattered intensities by molecules in all possible orientations.

The molecule form factor  $F_M$ , (1.52), is calculated by adding up the contributions of all  $N_{at}$  molecule atoms, whose relative positions do not change (rigid molecules) and the redistributions of electrons in chemical bonds are neglected. The intensity scattered by a single molecule is then given by

$$I_M(\mathbf{Q}) = I_{Th} |F_M(\mathbf{Q})|^2 = I_{Th} \sum_{a=1}^{N_{at}} \sum_{b=1}^{N_{at}} f_a(\mathbf{Q}) f_b^*(\mathbf{Q}) e^{i\mathbf{Q} \cdot \mathbf{r}_{ab}}. \quad (2.4)$$

In a disperse system of  $N$  molecules, the scattered intensity outside the direct beam would be  $N I_M(\mathbf{Q})$  if all molecules had the same spatial orientation. By the very fact that the system is sufficiently dispersed so that the molecules do not influence each other, the molecules have random orientations and all orientations with the same probability. The measurable intensity thus represents the average value of  $I_M$ ,

$$I(\mathbf{Q}) = N \langle I_M(\mathbf{Q}) \rangle = N I_{Th} \sum_{a=1}^{N_{at}} \sum_{b=1}^{N_{at}} f_a(\mathbf{Q}) f_b^*(\mathbf{Q}) \langle e^{i\mathbf{Q} \cdot \mathbf{r}_{ab}} \rangle \quad (2.5)$$

is the coherent intensity scattered by the disperse system of  $N$  molecules randomly oriented. The interatomic distances  $r_{ab}$  inside the molecules are fixed for each pair of atoms, and the average is calculated over all orientations of these interatomic distances with respect to the reciprocal vector. The averaging is similar to the angular part solution of the integral in Exercise 1.6(a), i.e.,

$$\mathbf{Q} = Q\hat{\mathbf{z}} = [0, 0, Q], \quad \mathbf{r}_{ab} = r_{ab} [\sin \gamma \cos \varphi, \sin \gamma \sin \varphi, \cos \gamma],$$

$$\mathbf{Q} \cdot \mathbf{r}_{ab} = Q r_{ab} \cos \gamma, \quad \text{and}$$

$$\begin{aligned} \langle e^{i\mathbf{Q} \cdot \mathbf{r}_{ab}} \rangle &= \frac{1}{4\pi} \int_0^{2\pi} \int_0^\pi [\cos(Qr_{ab} \cos \gamma) + i \sin(Qr_{ab} \cos \gamma)] \sin \gamma \, d\gamma \, d\varphi = \\ &= \frac{1}{2Qr_{ab}} \underbrace{\int_{-Qr_{ab}}^{+Qr_{ab}} (\cos w + i \sin w) \, dw}_{\text{where } w=Qr_{ab} \cos \gamma} = \frac{\sin(Qr_{ab})}{Qr_{ab}}. \end{aligned}$$

---

<sup>3</sup> Assuming X-ray beams with finite coherence lengths.

Thus,

$$I(Q) = N \langle I_M(Q) \rangle = N I_{Th} \sum_{a=1}^{N_{at}} \sum_{b=1}^{N_{at}} f_a(Q) f_b^*(Q) \frac{\sin(Qr_{ab})}{Qr_{ab}} = N I_{Th} P(Q). \quad (2.6)$$

For the sake of calculation efficiency, since  $r_{ab} = r_{ba}$ , the molecule's scattering power is rewritten as follows:

$$P(Q) = \sum_{a=1}^{N_{at}} |f_a(Q)|^2 + 2 \sum_{a=1}^{N_{at}-1} \sum_{b>a}^{N_{at}} \operatorname{Re}\{f_a(Q) f_b^*(Q)\} \frac{\sin(Qr_{ab})}{Qr_{ab}}, \quad (2.7)$$

so as to avoid double computing of the contribution of each atom pair. The sine function in the second term of  $P(Q)$  appears solely due to the interference phenomenon between the molecule atoms, implying in a modulation of the scattered intensity as a function of  $Q$ .

The existence of an interference pattern in the scattering curve is more evident when evaluating the scattering curve normalized by  $N I_{Th} \sum_a |f_a(Q)|^2$ , the intensity that would be scattered by the system in case of total absence of interference owing to the atomic structure of each molecule. The interference pattern is thus characterized by the structural function

$$\begin{aligned} S(Q) &= \frac{I(Q)}{N I_{Th} \sum_a |f_a(Q)|^2} = \frac{P(Q)}{\sum_a |f_a(Q)|^2} = \\ &= 1 + \frac{2}{\sum_a |f_a(Q)|^2} \sum_a \sum_{b>a} \operatorname{Re}\{f_a(Q) f_b^*(Q)\} \frac{\sin(Qr_{ab})}{Qr_{ab}}, \end{aligned} \quad (2.8)$$

which has a maximum value equal to or slightly smaller than  $N_{at}$  at  $Q = 0$ , i.e.  $S(Q = 0) \lesssim N_{at}$ , and oscillates around the unit for  $Q \rightarrow \infty$ .

...

**Exercise 2.2.** Consider a gas composed only of  $N$  benzene molecules,  $C_6H_6$ . (a) Neglecting the hydrogens, what is the structural function for this molecule? (b) Compare the intensity pattern of the gas with the one scattered by a single molecule in Fig. 1.13. (c) Decompose the interference pattern in the individual contributions of the molecule's characteristic interatomic distances. Which distance has greater weight? (d) How significant is the Compton scattering?

Answer (a): For a continuous distribution of orientations,

$$I(Q) = N I_{Th} 6 |f_C(Q)|^2 \overbrace{\left[ 1 + 2 \frac{\sin(Qd)}{Qd} + 2 \frac{\sin(Qd\sqrt{3})}{Qd\sqrt{3}} + \frac{\sin(2Qd)}{2Qd} \right]}^{S(Q)} =$$

$$= N \Phi r_e^2 \langle |\mathcal{P}(\hat{s}')|^2 \rangle d\Omega 6 |f_C(Q)|^2 S(Q)$$

is the intensity scattered by  $N$  molecules and  $S(Q)$  is the structural function.

Answer (b): By using the same cylindrical detector geometry shown in Fig. 1.12,

$$Q(z, \phi) = \frac{2\pi\sqrt{2}}{\lambda} \left( 1 - \frac{D \cos \phi}{\sqrt{D^2 + z^2}} \right)^{1/2}.$$

$\langle |\mathcal{P}(\hat{s}')|^2 \rangle$  and  $d\Omega$  are those used in Exercise 1.9. Figure 2.2a shows the intensity pattern for the gas. It is highly concentrated around the direct beam and has much less details than the pattern for a single molecule in Fig. 1.14. However, the movement of the molecules does not affect the measureable intensities, allowing long exposures and improving statistical resolution of the scattering curve outside the direct beam. In practice the resolution is limited by background radiation (Compton) and by the dynamic range<sup>4</sup> of the radiation detector.

Answer (c): In the benzene molecule, the interference pattern given by the structural function  $S(Q)$  is defined by the superposition of three functions of the type  $\sin(Qd)/Qd$ , concerning to the distances  $d = 140, 243$ , and  $280$  pm, as shown in Fig. 2.2b. The weights are 2, 2, and 1, respectively.

Answer (d): To include the Compton scattering in Fig. 2.2a:

$$I(Q) = N I_{Th} 6 [|f_C(Q)|^2 S(Q) + S(Z, Q)]$$

where the function  $S(Z, Q)$  is given by (1.56), with  $Z = 6$  in the case of carbon. For 20 keV photons, Compton becomes more significant than the coherent scattering, i.e.  $S(Z, Q) > |f_C(Q)|^2 S(Q)$ , when  $Q > 3.5 \text{ \AA}^{-1}$  ( $2\theta > 20^\circ$ ).

...

---

<sup>4</sup>Useful range of a radiation detector in intensity scales or dose per pixel.

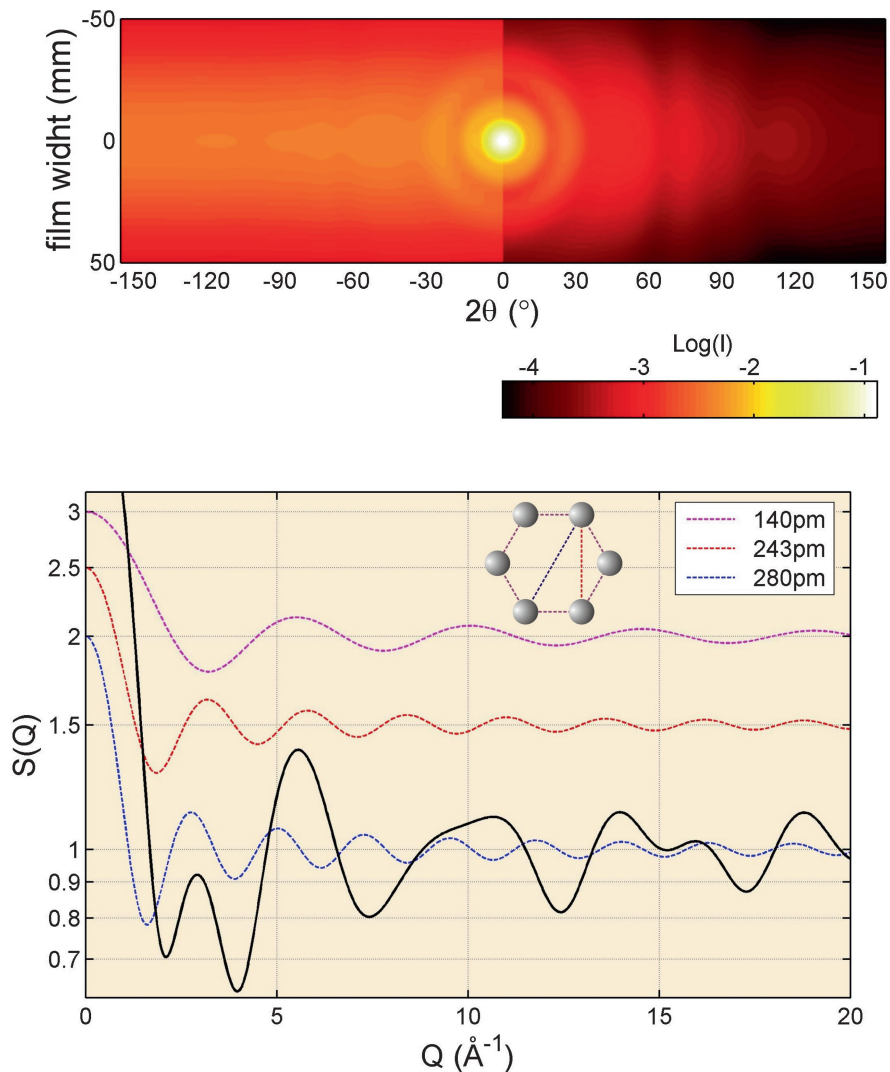


**Fig. 2.2** (Top) Intensity scattered by  $N$  benzene molecules with random orientations. The background intensity from Compton scattering is considered only for carbon atoms and negative values of  $2\theta$ . X-rays of 20 keV, sample-film distance  $D = 50$  mm,  $\sigma$  polarization, and flux so that  $N\Phi r_e^2 = 1$  cps. (Bottom) Function  $S(Q)$  (black line) for the benzene molecule,  $S(0) = 6$ . The individual contributions (dashed curves) of the three characteristic interatomic distances in the molecule are displaced in the ordinate axis for better viewing [benzenesaxs1.m, benzenesaxs2.m]



## 2.3 Small Angle Scattering

The analysis of  $S(Q)$  in the large  $Q$  region would provide, in principle, information on minor values of  $r_{ab}$ . However, there are several experimental difficulties to access such information, one of them imposed by the maximum value of  $Q$  that is limited by the radiation energy, usually in the order of a few tens of keV, (1.49). This implies that, when studying disperse systems by X-ray scattering, the information on the smaller interatomic distances, in scale of angstrom, are only accessible at high angles, just where the atomic scattering factors are very reduced in comparison with the values at small angles and the Compton scattering is more intense, as can be seen in Fig. 1.16. Since low density of molecules and absence of long-range order are inherent properties of disperse systems, measurements with satisfactory statistical resolution of the coherent scattered intensity at high angles are most times impracticable in these systems.

On the other hand, measures of scattered intensity in the small  $Q$  region provide information about the largest interatomic distances of the order of physical dimensions of the molecules. To demonstrate this property of the small angle scattering, we take the limit of (2.6) when  $Qr_{ab} \rightarrow 0$  so that

$$\begin{aligned} I(Q) &\approx N I_{Th} \sum_{a=1}^{N_{at}} \sum_{b=1}^{N_{at}} f_a(Q) f_b^*(Q) \left[ 1 - \frac{1}{6} (Qr_{ab})^2 \right] \\ &\approx N I_{Th} f_m^2(0) \sum_{a=1}^{N_{at}} \sum_{b=1}^{N_{at}} \left[ 1 - \frac{1}{6} (Qr_{ab})^2 \right] = N I_{Th} f_m^2(0) N_{at}^2 \left( 1 - \frac{1}{3} Q^2 \langle r^2 \rangle \right). \end{aligned}$$

To get to the equation above, use

$$\lim_{x \rightarrow 0} \frac{\sin x}{x} \simeq \frac{x - x^3/6}{x} = 1 - \frac{1}{6} x^2$$

and replace  $f_a(Q) f_b^*(Q)$  with  $f_m^2(0)$  since  $N_{at}^2 f_m^2(0)$  is the value of the summation when  $Q = 0$ , or for a more general definition:  $f_m^2(Q) = N_{at}^{-2} \left| \sum_a f_a(Q) \right|^2$ . Recalling that  $e^{-x} \simeq 1 - x$  for  $x \ll 1$ , we obtain the intensity expression in the limit as  $Q$  approaches zero,

$$\lim_{Q \rightarrow 0} I(Q) = N I_{Th} f_m^2(0) N_{at}^2 e^{-\frac{1}{3} Q^2 \langle r^2 \rangle}. \quad (2.9)$$

$$\langle r^2 \rangle = \left( \frac{1}{2} \sum_{a=1}^{N_{at}} \sum_{b=1}^{N_{at}} r_{ab}^2 \right) / N_{at}^2 = \left( \sum_{a=1}^{N_{at}-1} \sum_{b>a}^{N_{at}} r_{ab}^2 \right) / N_{at}^2 \quad (2.10)$$

is the molecule mean square radius, thus demonstrating that the scattered intensity at small  $Q$  region is determined by the size of the molecules. The root-mean-square radius  $R_g = \sqrt{\langle r^2 \rangle}$  is commonly called radius of gyration of the molecule.

### 2.3.1 Macromolecules

The atom-by-atom description is not restricted to cases of simple molecules. Thanks to the current computational facilities, exact calculations of both the radius of gyration and intensity are feasible even for giant molecular complexes containing tens of thousands of atoms. The protein database is one of the largest sources available on discrete structures (atom-by-atom). When a protein has its structure determined, in general by X-ray diffraction in the crystallized protein, it is available at the *Protein Data Bank* (<http://www.pdb.org/>). Among other format options, there are text files (\*.pdb) in standard pdb format where the atomic coordinates are given in the lines starting with “ATOM” or “HETATM,” such as

```

-----
ATOM      84  N   LYS  A   12      55.325  15.647  18.827  1.00 19.22      N
ATOM      85  CA  LYS  A   12      55.370  17.014  18.328  1.00 22.23      C

      . . .
HETATM 4716  C14 MYR  A1006      29.904   5.219  -4.802  1.00 48.47      C
HETATM 4717  FE  HEM  A   605      32.347   8.521  32.831  1.00 25.18      FE
-----
column: 1234567890123456789012345678901234567890123456789012345678901234567890
          1           2           3           4           5           6           7           8

```

where the atom with sequential number 85 is a carbon of the amino acid lysine (LYS) with coordinates  $X = 55.370 \text{ \AA}$  (columns 31–38),  $Y = 17.014 \text{ \AA}$  (columns 39 to 46), and  $Z = 18.328 \text{ \AA}$  (columns 47–54). The symbol of the chemical element is given in columns 77 and 78. For more details about the pdb standard, see the file-format documentation also available at the pdb website.

In the Appendix B, the `saxs.c` routine written in C++ reads files in pdb format and returns  $P(Q)$ ,  $S(Q)$ , and  $R_g$  calculated according to (2.7), (2.8), and (2.10), respectively. Although the calculation of  $P(Q)$  through (2.7) is exact for any  $Q$ , it is a method of small computational efficiency. Later we will take a look at some approaches that make the calculation much more efficient and executable in MatLab™ in the experimentally accessible region of  $Q$  (small angle), but it will be interesting to have the exact calculation for the sake of comparison.

...

**Exercise 2.3.** With the known structure of a protein (file \*.pdp), calculate its scattering power,  $P(Q)$ , and radius of gyration. (a) What is the mean number of electrons per atom effectively scattering X-rays? Relate this number with the expected value of  $P(0)$ . Note: despise hydrogens and chemical bonds, use  $f_a(Q)$  for neutral atoms. (b) Which region of the  $P(Q)$  curve has exponential decay with  $Q^2$ ?

Answer (a): From (2.6) follows  $P(0) = \left| \sum_a^{N_{at}} f_a(0) \right|^2$ . Since at  $Q = 0$  all the electrons scatter in phase, the mean effective number of electrons per atom is  $f_m(0) = N_{at}^{-1} \sqrt{P(0)}$ . In the case of the protein shown in Fig. 2.3, there are 4635 atoms (“ATOM” records in the 1N5U.pdb file): 784 N, 2926 C, 884 O, and 41 S.  $P(0) = |784f_N(0) + 2926f_C(0) + 884f_O(0) + 41f_S(0)|^2 \simeq 9.469 \times 10^8$  if atomic

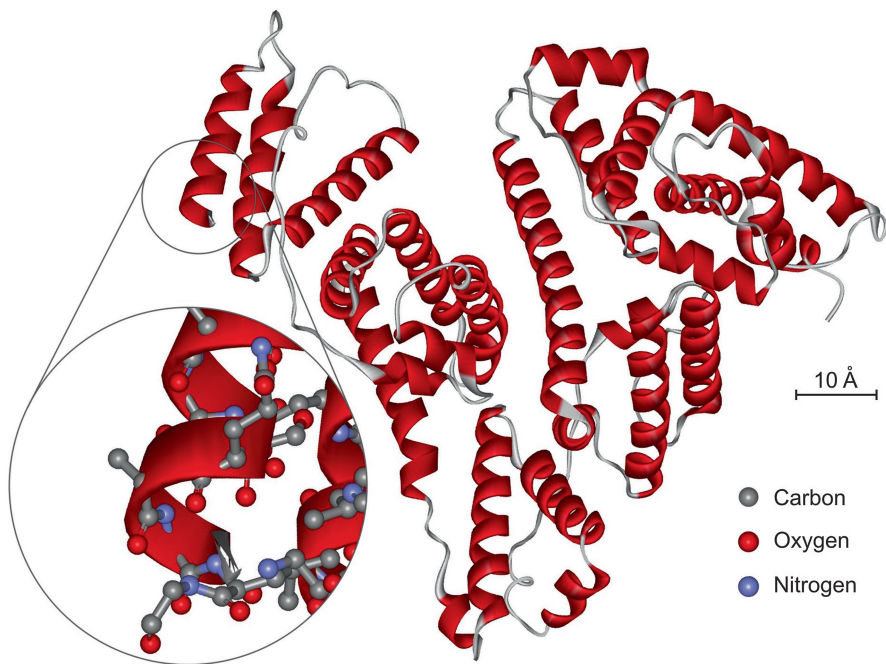


**Fig. 2.3** Amino acid chains of human albumin, protein 1NSU in the *Protein Data Bank* (<http://www.pdb.org/>)

resonances are neglected, otherwise  $P(0) = 9.547 \times 10^8$  for X-ray photons of 8 keV. So there are  $f_m(0) = 6.6665$  effective electrons per atom.

Answer (b): In Fig. 2.4,  $P(Q) = P(0) \exp(-\frac{1}{3}R_g^2 Q^2)$  from  $Q = 0$  to approximately  $Q = 0.08 \text{ \AA}^{-1}$  ( $Q^2 = 0.0064 \text{ \AA}^{-2}$ ) where the value of  $R_g = 27.9 \text{ \AA}$  was obtained by (2.10).

### 2.3.2 Particles of Uniform Density

Scattering properties in the region of small  $Q$  can be obtained in an equivalent manner to that shown for discrete molecules, starting from the assumption of particles of uniform density. When we look at the radiation scattered in a small enough angle so that the interatomic distances do not affect the scattering of X-rays, the electron density is rewritten as

$$\rho(\mathbf{r}) = \frac{F_M(0)}{v_p} s(\mathbf{r}) \simeq \frac{N_{at} f_m(0)}{v_p} s(\mathbf{r}) = \bar{\rho} s(\mathbf{r}) . \quad (2.11)$$

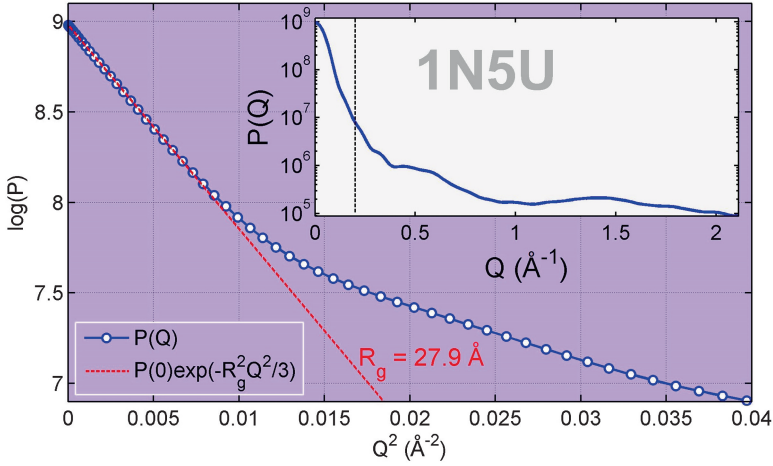


**Fig. 2.4** Log( $P$ ) curve versus  $Q^2$  in the region  $Q < 0.2 \text{ \AA}^{-1}$  for human albumin (PDB ID: 1N5U). *Inset:* scattering power in an extended region of  $Q$  [saxs.c, ex1N5U.m]

$s(\mathbf{r})$  is the shape function:  $s = 1$  (or 0) for  $\mathbf{r}$  inside (or outside) of the particle outline.  $F_M(0) = \sum_a^{N_{at}} f_a(0) \simeq N_{at} f_m(0) = |\sum_a^{N_{at}} f_a(0)|$  is the effective number of electrons in the particle of volume  $v_p$ , so that  $\bar{\rho} = N_{at} f_m(0)/v_p$  is the average density of electrons in the particle effectively scattering radiation. Thus, the new particle form factor for small angles, including cases of particles dispersed in a homogeneous medium with electron density  $\rho_0$ , is

$$F'_M(\mathbf{Q}) = (\bar{\rho} - \rho_0) \text{FT}\{s(\mathbf{r})\}. \quad (2.12)$$

Since the measurable intensity is the average  $\langle \dots \rangle$  on all possible particle orientations, we have

$$I(Q) \simeq N I_{Th} \langle |F'_M(\mathbf{Q})|^2 \rangle = N I_{Th} (\bar{\rho} - \rho_0)^2 \langle |\text{FT}\{s(\mathbf{r})\}|^2 \rangle = N I_{Th} P(Q) \quad (2.13)$$

where the scattering power  $P(Q)$  depends only on the particle shape and its density contrast with the medium.

The technique known as small angle X-ray scattering (SAXS) is widely used in the study of low correlated systems, particularly those systems where the particles have sizes in the range of 1–50 nm. Typically,  $0.1^\circ < 2\theta < 10^\circ$  corresponds to the angular range analyzed by SAXS, depending on the particularities of each instrumental setup (Craievich 2002).

### 2.3.3 Morphology of Particles

The approach of uniform density is valid within a restricted range of reciprocal space ranging from  $Q = 0$  to a certain value of  $Q$ , from which the scattering curve starts to be affected by the density fluctuations inside the particle. Around the direct beam, in the so-called Guinier region, this approach is very good. The intensity curve always shows the exponential decay with  $Q^2$ , as given by (2.9), which in terms of average density is

$$\lim_{Q \rightarrow 0} I(Q) = N I_{Th} (\bar{\rho} - \rho_0)^2 \lim_{Q \rightarrow 0} \langle |\text{FT}\{s(\mathbf{r})\}|^2 \rangle = N I_{Th} (\bar{\rho} - \rho_0)^2 v_p^2 e^{-\frac{1}{3} Q^2 \langle r^2 \rangle} \quad (2.14)$$

where

$$\langle r^2 \rangle = \frac{1}{v_p} \int_{v_p} r^2 dV \quad (2.15)$$

is the mean square radius,<sup>5</sup> equivalent to that obtained by the discrete summation in (2.10), but with the advantage of being calculated from the particle shape without the need for prior knowledge of the interatomic distances. For example, for a spherical particle of radius  $a$ ,

$$R_g^2 = \langle r^2 \rangle = 3a^2/5 \quad \text{and} \quad I(Q)/I(0) = e^{-0.2 (Qa)^2}.$$

Note that this is almost the same result of the exponential decay  $e^{-0.21 (Qa)^2}$  used to adjust the initial part of the scattered intensity curve by a spherical and uniform electron density in Exercise 1.6(b); the slight difference arises from the fact that in the Exercise the scattering at half maximum was used as reference,  $I(Qa=1.815)/I(0) = 1/2$ , rather than the limit for  $Q \rightarrow 0$ .

The intensity curve range that can be reproduced by an exponential decay with  $Q^2$  varies with the particle morphology. In most cases, it goes from  $Q = 0$  to a value not far beyond  $Q = 1/R_g$ . This value serves as an estimate of the extent of Guinier region in the intensity curve, from which only information on particle size (radius of gyration) can be extracted.

After the Guinier region, the exponential decay with  $Q^2$  is replaced by a behavior strongly influenced by the particle shape. The extent at  $Q$  of this region with particle's morphological information, which is often called Porod region (Guinier 1994), depends on how much larger are the dimensions of the particle in relation to the scale length of the internal density fluctuations. Due to the wide variety of

---

<sup>5</sup>It is an optional task to demonstrate that  $\lim_{Q \rightarrow 0} \langle |\text{FT}\{s(\mathbf{r})\}|^2 \rangle = v_p^2 e^{-\frac{1}{3} Q^2 \langle r^2 \rangle}$ . Such demonstration can be found in several books on SAXS, e.g. Giacobazzo (2002), Glatter and Kratky (1982), and Guinier (1994).

systems it is difficult to establish a general rule for the occurrence or not of the Porod region. However, as a rule, it is expected that the morphological analysis is feasible when the particle is dozens of times larger than the size of the molecules composing it.

In the case of particles of uniform density, abrupt interfaces and regular surfaces, (2.13) foresees intensity curves with asymptotic fall of the type  $1/Q^n$  where  $n$  is an integer<sup>6</sup> related to the dimensionality of the particle. Analytical solutions for the term  $\langle |\text{FT}\{s(\mathbf{r})\}|^2 \rangle$  are possible for specific types of particles, while numerical solutions are necessary in most cases, see, for example, Lindner and Zemb (2002). Here we will make a simple, but quite versatile, numerical approach to demonstrate the main features of the asymptotic behavior in the intensity curves. This demonstration is based on the fact that (2.6) and (2.13) provide nearly the same results in the  $Q$  range comprising both Guinier and Porod regions, i.e.

$$I(Q)/I(0) = \frac{1}{V^2} \langle |\text{FT}\{s(\mathbf{r})\}|^2 \rangle \simeq \frac{2}{N(N-1)} \sum_a^{N-1} \sum_{b>a}^N \frac{\sin(Qr_{ab})}{Qr_{ab}} \quad (2.16)$$

as long as the position vectors  $\mathbf{r}$  are uniformly distributed within the particle shape (outline) and in sufficient quantity so that the  $r_{ab}$  values of adjacent positions are much smaller than the dimensions of the particle.

Through (2.16), using random distributions of position vectors within the chosen particle shape, the following asymptotic behaviors can be verified. Particles with dimension 3 where the ratio between dimensions in three orthogonal directions tends to 1 : 1 : 1, such as spheres and cubes, the intensity of the interference fringes falls with  $1/Q^4$ ,  $n = 4$ , Fig. 2.5. In the case of spherical particles, the fall with  $1/Q^4$  can be verified analytically from the FT of a sphere, as calculated in Exercise 1.6(b). Sharp reduction in one or two dimensions of the particle eliminates the interference fringes in the Porod's region and changes the value of  $n$ . Particles with dimension 2 are those with a planar aspect for which  $n = 2$ ,  $1/Q^2$  asymptote. Those with elongated aspects, rod-type, have dimension 1 for which  $n = 1$ ,  $1/Q$  asymptote. Figure 2.5 also shows the theoretical scattering curves of particles with ratios 1:1: $w$  (dimension 2) and  $w:w:1$  (dimension 1) in the limit  $w \rightarrow 0$ . Curves with asymptotes  $1/Q^n$  for larger  $Q$  values occur when the particle dimensional aspect (3, 2 or 1) is well defined, i.e. at the  $w = 0$  and  $w = 1$  limits (solid line curves in Fig. 2.5). In intermediate cases, the range where the  $1/Q^n$  behavior occurs is less and less the more the particle proportions deviate from the limiting cases (dashed line curves in Fig. 2.5).

...

---

<sup>6</sup>Non-integer values occur in particles without defined interfaces, such as macromolecules and materials with fractal properties (Teixeira 1988).

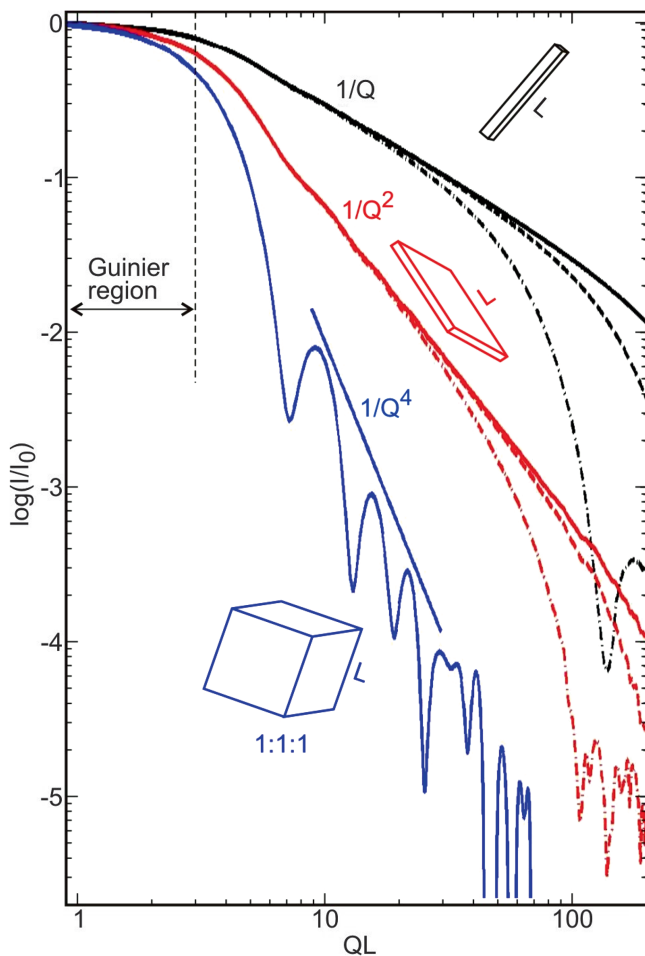


**Fig. 2.5** Asymptotic behavior of the intensity scattered by particles with different dimensionalities: 1:1:1 (dimension 3), 1:1: $w$  (dimension 2), and  $w:w:1$  (dimension 1) where  $w = 1/100$  (straight line),  $2/100$  (dashed line), and  $5/100$  (dashed with dotted line). Curves calculated numerically by using (2.16) with  $N = 2000$  [assintotic.m]

**Exercise 2.4.** Particles of uniform density and spheroidal shapes. (a) How does the radius of gyration  $R_g$  depend on oblate and prolate shapes? (b) When does  $R_g$  cease to depend on the ratio  $w$  between the smallest and largest dimensions of the particle? Answer (a): By writing (2.15) in cylindrical coordinates  $(\rho, \phi, z)$ ,

$$\langle r^2 \rangle = \frac{2\pi}{v_p} \int_{-c}^c \int_0^{\rho(z)} (\rho'^2 + z^2) \rho' d\rho' dz.$$

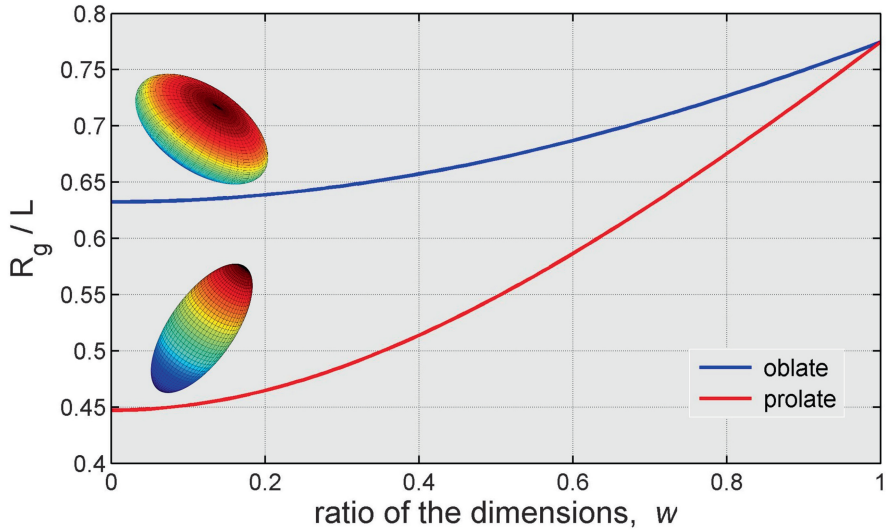


**Fig. 2.6** Radius of gyration  $R_g$  as a function of ratio  $w$  between the smallest and the largest dimension ( $2L$ ). Particles of uniform density and spheroidal shapes,  $w = 1$  implies sphere of radius  $L$  [exellipsoid.m]

From the equation of an ellipsoid of revolution,  $(x/a)^2 + (y/a)^2 + (z/c)^2 = 1$ , we have  $\rho^2(z) = a^2[1 - (z/c)^2]$  and  $v_p = 4\pi a^2 c/3$ . The analytical solution of the integral leads to  $\langle r^2 \rangle = (2a^2 + c^2)/5$ . Oblate shapes:  $a = L$ ,  $c = wL$  where  $w < 1$ , and  $R_g^2 = (2 + w^2)L^2/5$ . Prolate shape:  $c = L$ ,  $a = wL$ , and  $R_g^2 = (2w^2 + 1)L^2/5$ . Answer (b): From the  $R_g \times w$  graph, Fig. 2.6, it can be seen that for  $w < 0.1$ ,  $R_g$  is already close to the limit values:  $\sqrt{2/5} L$  (oblates) and  $\sqrt{1/5} L$  (prolates).

...

**Suggestion:** Calculate the scattering curve by using (2.16) in the Guinier region and numerically obtain the radius of gyration for particles with different dimensionalities.

...

### 2.3.4 Polydisperse Systems and Dispersion of Size

The kinematic intensity in polydisperse systems, i.e. composed by different particles without interacting with each other, can be treated as the sum of the intensities of monodisperse systems, (2.6) or (2.13). So,  $I(Q) = I_{Th} \sum_j N_j P_j(Q)$  where the index  $j$  specifies each of the independent systems that comprise the total system



(polydisperse). Within the approaching of particles of uniform density in a solvent of electronic density  $\rho_0$ ,  $P_j(Q) = (\bar{\rho}_j - \rho_0)^2 \langle |\text{FT}\{s_j(\mathbf{r})\}|^2 \rangle$  and weight

$$C_j(0) = N_j P_j(0) = N_j (\bar{\rho}_j - \rho_0)^2 v_{p,j}^2$$

of the contribution of each system  $j$  in the scattered intensity is determined by the number  $N_j$  of particles  $j$ , and their scattering power in relation to the media. The intensity in polydisperse systems in the limit  $Q \rightarrow 0$  remains

$$I(Q) = I(0) e^{-\frac{1}{3} Q^2 R_g^2},$$

but the radius of gyration is given by

$$R_g^2 = \frac{\sum_j C_j(0) \langle r^2 \rangle_j}{\sum_j C_j(0)} \quad (2.17)$$

where  $\langle r^2 \rangle_j$  is the mean square radius of the  $j$  particles, and  $I(0) = I_{Th} \sum_j C_j(0)$ .

A very common type of polydisperse system found in many real situations is the one formed by particles with the same electronic density  $\bar{\rho}$ , but presenting variations in shape and size. This allows rewriting the expression of intensity as

$$I(Q) = I_{Th} (\bar{\rho} - \rho_0)^2 \sum_j N_j \langle |\text{FT}\{s_j(\mathbf{r})\}|^2 \rangle. \quad (2.18)$$

In the most general cases of particles having different morphologies, the analysis of scattering curves is often infeasible. On the other hand, when the particles have the same shape, e.g. spherical particles embedded in a homogeneous liquid or solid matrix, the dispersion of size softens the interference fringes that normally occur in the intensity curve, making it easier to analyze the asymptotic behavior in the Porod region. Determining the size distribution (point of interest in research involving many nanoparticle synthesis) is possible under certain circumstances. When the shape function depends only on the dimensional variable  $L$  of the particle,  $s_j(\mathbf{r}) \rightarrow s(L, \mathbf{r})$  and  $N_j \rightarrow N p(L) dL$  where  $N$  is the total number of particles in the system and  $p(L)$  is the size distribution function so that  $\int_0^\infty p(L) dL = 1$ . The intensity in (2.18) is thus given by the integral

$$I(Q) = N I_{Th} (\bar{\rho} - \rho_0)^2 \int_0^\infty p(L) \langle |\text{FT}\{s(L, \mathbf{r})\}|^2 \rangle dL, \quad (2.19)$$

and the radius of gyration in (2.17) becomes

$$R_g^2 = \frac{\int_0^\infty p(L) v_p^2(L) R_g^2(L) dL}{\int_0^\infty p(L) v_p^2(L) dL}. \quad (2.20)$$

$R_g(L)$  is the radius of gyration of the particles whose value of dimensional variable is between  $L$  and  $L + dL$ .

Intensity curves with asymptotes  $1/Q^4$  are associated with regular particles without surface fractality and without sharply planar or linear character—ratio between smallest and largest size a lot greater than  $1/10$ . In such cases, it is possible to show that the integral in (2.19) is

$$N \int_0^\infty p(L) \langle |\text{FT}\{s(L, \mathbf{r})\}|^2 \rangle dL \simeq \frac{2\pi}{Q^4} N \int_0^\infty p(L) A_s(L) dL = 2\pi \frac{N \langle A_s \rangle}{Q^4} = 2\pi \frac{A}{Q^4} \quad (2.21)$$

in the region where the interference fringes are softened by the size distribution  $p(L)$ .  $A_s(L)$  is the surface area of the particles with size  $L$ , and  $A = N \langle A_s \rangle$  is the total surface area of the  $N$  particles, corresponding to the total area of the interface between particles and solvent, that is, between materials with densities  $\bar{\rho}$  and  $\rho_0$ .

$$I(Q) = 2\pi I_{Th} (\bar{\rho} - \rho_0)^2 \frac{A}{Q^4} \quad (2.22)$$

is known as the Porod's law and can be observed in several systems consisting of materials with two different electron densities (Craievich 2002).

...

**Exercise 2.5.** Spherical particles, besides being analytically tractable, quite often occur in the synthesis of nanoparticles. Considering a disperse system of spherical particles with continuously distributed radius around a most likely value  $a_0$ . (a) Make the theoretical demonstration<sup>7</sup> of Porod's law in (2.22). (b) What is the relationship between visibility of the fringes and dispersion of size (radius)?

Answer (a): When  $s(L, \mathbf{r})$  is the shape function of a spherical particle of radius  $a$ , it follows from (1.38) that

$$\begin{aligned} \langle |\text{FT}\{s(L, \mathbf{r})\}|^2 \rangle &= v_p^2(a) \Theta^2(Qa) = (4\pi a^3)^2 \left[ \frac{\sin(Qa) - (Qa) \cos(Qa)}{(Qa)^3} \right]^2 = \\ &\simeq 8\pi^2 \left[ \frac{a^2}{Q^4} + \frac{1}{Q^6} + \left( \frac{a^2}{Q^4} - \frac{1}{Q^6} \right) \cos(2Qa) - \frac{2a}{Q^5} \sin(2Qa) \right]. \end{aligned}$$

Discarding terms with  $Q^{-5}$  and  $Q^{-6}$ , and substituting this expression in (2.19) with the radius  $a$  in the place of the dimensional variable  $L$ ,

---

<sup>7</sup>See Guinier (1994, p. 336).

$$I(Q) \simeq I_{Th} (\bar{\rho} - \rho_0)^2 \frac{2\pi N}{Q^4} \int p(a) 4\pi a^2 [1 + \cos(2Qa)] da \simeq 2\pi I_{Th} (\bar{\rho} - \rho_0)^2 \frac{A}{Q^4}.$$

The higher the dispersion of size distribution and the  $Q$  values, the more the cosine contributions tend to cancel each other so that  $\int p(a) 4\pi a^2 \cos(2Qa) da \simeq 0$ , thus leading to the Porod's formula (or law) as we wanted to demonstrate.

Answer (b): Fringes are no longer visible when  $\cos(2Qa)$  ranges from  $-1$  to  $+1$  within a small range of the  $a$  values, i.e. when  $Q > \pi/\Delta a$  where  $\Delta a$  represents the dispersion of values such as the full width at half maximum of the distribution  $p(a)$ .

**Exercise 2.6.** Consider a non-Gaussian distribution of spherical particles. (a) Simulate the scattering curve. From what value of  $Q$  does the curve become smooth (without fringes)? (b) Compare values of gyration radius  $R_g$  and average surface area  $\langle A_s \rangle$  with those obtained by Gaussian distributions capable of generating similar scattering curves. In what circumstances is it possible to clearly distinguish between Gaussian and non-Gaussian size distributions?

Answer (a): One of the most common non-Gaussian distribution is the log-normal distribution

$$p(a) = \frac{1}{a \sigma_n \sqrt{2\pi}} e^{-(\ln a - \ln b)^2 / 2\sigma_n^2},$$

whose variable  $b = a_0 e^{\sigma_n^2}$  depends on the value of  $a_0$  (most probable radius) and of the standard deviation in logarithmic scale,  $\sigma_n$ . As expected, Exercise 2.5(b), the fringes disappear for  $Q > \pi/\Delta a$  where  $\Delta a$  is the full width at half maximum of  $p(a)$ . As for example, the two distributions shown in Fig. 2.7 (inset),  $\Delta a = 23.5 \text{ \AA}$  and  $36.3 \text{ \AA}$ , which implies that the regions without fringes have  $Q > 0.13 \text{ \AA}^{-1}$  and  $Q > 0.08 \text{ \AA}^{-1}$ , respectively.

Answer (b): Let  $p(a) = \frac{1}{\sigma \sqrt{2\pi}} e^{-(a-a_0)^2 / 2\sigma^2}$  be the Gaussian distribution used for the sake of comparison.<sup>8</sup> In Table 2.1, the parameters of the two distributions resulting in similar curves are compared. The values are no longer compatible when the log-normal distribution is very asymmetric. However, in these cases  $\sigma \gtrsim a_0/3$ , implying in a significant fraction of particles with null radius ( $a = 0$ ), a fact that can be used as a feasibility criterion of the Gaussian model for describing the size distribution.

...

<sup>8</sup>For large values of  $\sigma$ , such as  $\sigma > a_0/3$ , the normalization constant is reset so that  $\int_0^\infty p(a) da = 1$ .

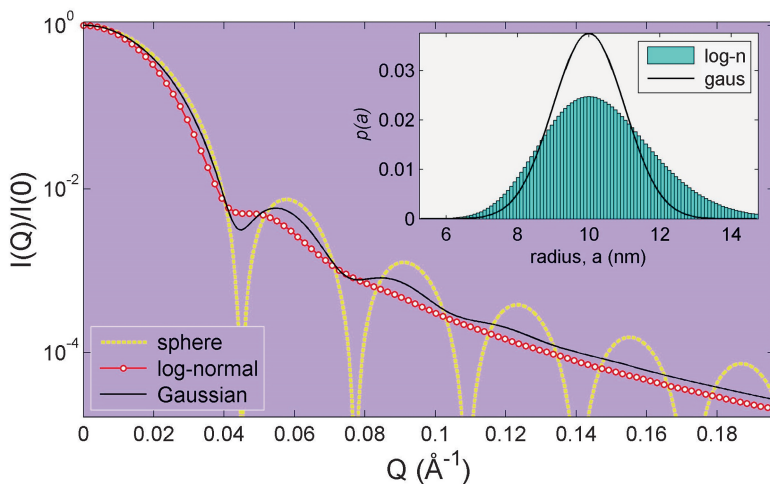


**Fig. 2.7** Normalized intensity curves of X-ray scattering by disperse systems of spheres with uniform density and different size distributions (*inset*). Reference curve of the scattering by spheres of radius  $a_0$  (most probable radius of the distributions) is also shown [exlognormal.m]

**Table 2.1** Parameters of the log-normal and Gaussian size distributions producing similar scattering curves

$a_0$ (Å)	Log-normal			Gaussian		
	$\sigma_n$	$R_g$ (Å)	$\langle A_s \rangle$ (Å <sup>2</sup> )	$\sigma$ (Å)	$R_g$ (Å)	$\langle A_s \rangle$ (Å <sup>2</sup> )
50	0.1	42.0	$3.3 \times 10^4$	5.9	42.0	$3.2 \times 10^4$
50	0.2	53.2	$3.7 \times 10^4$	13.7	53.0	$3.4 \times 10^4$
100	0.3	153.5	$1.8 \times 10^5$	49	145.1	$1.6 \times 10^5$
100	0.7	1095	$8.8 \times 10^5$	397	850	$24.1 \times 10^5$

$R_g$  and  $\langle A_s \rangle$  calculated from (2.20) and (2.21), respectively. For comparison details see routine exlognormal.m

## Summary

— Scattering power of discrete particles:

$$P(Q) = \sum_a \sum_b f_a(Q) f_b^*(Q) \frac{\sin(Qr_{ab})}{Qr_{ab}}$$

— Scattering power of uniform particles in solution:

$$P(Q) = (\bar{\rho} - \rho_0)^2 \langle |\text{FT}\{s(\mathbf{r})\}|^2 \rangle$$

— Low angle approach, limit  $Q \rightarrow 0$ , Guinier region:

$$P(Q) = P(0) \exp\left(-\frac{1}{3}Q^2 R_g^2\right)$$

— Particle's gyration radius,  $R_g$ :

$$R_g^2 = \left(\frac{1}{2} \sum_a \sum_b r_{ab}^2\right) / N_{at}^2 \text{ (discrete)} \quad \text{or} \quad R_g^2 = \frac{1}{v_p} \int v_p r^2 dV \text{ (uniform)}$$

— Asymptotic behavior, regular uniform particles, Porod region:

$$P(Q) = 2\pi (\bar{\rho} - \rho_0)^2 A / Q^4$$

— Total surface area of particles with  $p(L)$  size distribution:

$$A = N \langle A_s \rangle = N \int_0^\infty p(L) A_s(L) dL$$

— Average gyration radius:

$$R_g^2 = \frac{\int_0^\infty p(L) v_p^2(L) R_g^2(L) dL}{\int_0^\infty p(L) v_p^2(L) dL}$$

— Size distributions:

$$p(L) = \frac{e^{-(L-L_0)^2/2\sigma^2}}{\sigma \sqrt{2\pi}} \text{ (Gaussian)} \quad \text{and} \quad p(L) = \frac{e^{-(\ln L - \ln b)^2/2\sigma_n^2}}{L \sigma_n \sqrt{2\pi}} \text{ (log-normal)}$$

$$b = L_0 \exp(\sigma_n^2)$$

Computer Simulation Tools for X-ray Analysis  
Scattering and Diffraction Methods

Morelhão, S.L.

2016, XV, 294 p., Hardcover

ISBN: 978-3-319-19553-7